Hindawi Publishing Corporation
Journal of Nanomaterials
Volume 2015, Article ID 613124, 6 pages
http://dx.doi.org/10.1155/2015/613124

Research Article

Palladium-Gold Nanoalloy Surface Modified $LiMn_2O_4$ Cathode for Enhanced Li-Ion Battery

Natasha Ross, Myra Nzaba, Wonderboy Ntuthuko, Chinwe Ikpo, Priscilla Baker, and Emmanuel Iwuoha

SensorLab, Department of Chemistry, University of Western Cape, Private Bag X17, Bellville, Cape Town 7535, South Africa

Correspondence should be addressed to Natasha Ross; nross@uwc.ac.za

Received 13 January 2015; Accepted 6 April 2015

Academic Editor: Wei Chen

Au with Pd nanoparticles were synthesized and coated onto the spinel $LiMn_2O_4$ via a coprecipitation calcination method with the objective to improve the microstructure, conductivity, and electrochemical activities of pristine $LiMn_2O_4$. The novel $Li[PdAu]_xMn_{2-x}O_4$ composite cathode had high phase purity, well crystallized particles, and more regular morphological structures with narrow size distributions. At enlarged cycling potential ranges the $Li[PdAu]_xMn_{2-x}O_4$ sample delivered 90 mAh g^{-1} discharge capacity compared to $LiMn_2O_4$ (45 mAh g^{-1}). It was concluded that even a small amount of the Pd and Au enhanced both the lithium diffusivity and electrochemical conductivity of the host sample due to the beneficial properties of their synergy.

1. Introduction

Lithium-ion batteries are becoming incredibly popular in modern electronic devices. Compared with traditional battery technology, lithium-ion batteries charge faster, with an operating voltage of ~3.7 V, last longer, and have a higher power density in a lighter package [1]. For the application of LIBs, the main concerns of electrochemical performance are cost reduction, cycle life, power density, energy density, and especially safety [2]. It has thus become particularly important to develop cathode materials with reversible and fast charge-transfer reactions in addition to high capacities. The most investigated and commercially used cathode materials include layered $LiCoO_2$ and $LiNiO_2$ [3], $LiNiVO_4$ and $LiCoVO_4$ [4], and $LiMnO_4$ [5]. Among these the spinel $LiMn_2O_4$ provides several advantages for Li-ion batteries because of their high voltage (4 V versus Li/Li+), good cyclability, lower cost of production, lower toxicity, and safety [6]. Depending on the synthetic procedure, nanosized $LiMn_2O_4$ with different desirable physical and chemical properties can be produced [7, 8]. Solid-state reaction is the most conventional method to prepare $LiMn_2O_4$, however with the disadvantage of large particle size, wide-ranging particle size distribution, and irregular morphology [9]. To overcome these disadvantages, a sustainable effort of many researchers has gone into the development of soft chemistry methods [10]. Hence, the coprecipitation technique is considered the simplest and most efficient chemical pathway to yield nanocrystalline $LiMn_2O_4$. However, $LiMn_2O_4$ still suffers from structural reconstruction and Mn dissolution in the electrolyte upon cycling, which results in high capacity fading [11]. Therefore, most research attempts to improve the electrochemical performance of the spinel have been directed toward the synthesis of cation-doped $LiMn_2O_4$ and surface passivation treatment [12, 13]. The elements commonly used for modification include nonmetals, rare-earth metals, and actinide dopants. These modification methods can weaken the Jahn-Teller effect, decrease the dissolution of active material, minimize surface overpotential, and stabilize the structure which concomitantly enhances the electrochemical performance of the cathode [14]. In this study, palladium is of interest from both fundamental and technological viewpoints because of quantum size effect, which is derived from the reduction of free electrons [15]. Likewise, gold and palladium bimetallic nanoparticles [16] have recently emerged as viable catalysts due to their unique properties. These properties include large binding energy and the potential to reduce Mn^{3+} content, increase the average valence of Mn, and

stabilize the cubic structure of $LiMn_2O_4$ compared to their bulk counterparts. In this communication, the use and beneficial synergistic effects of Pd-Au alloy as a novel $LiMn_2O_4$ surface coating material are reported. The correlation of $Li[PdAu]_xMn_{2-x}O_4$ on the electrochemical performance, crystal structure stability, and morphology is investigated and discussed.

2. Experimental Section

2.1. Synthetic Methodology of Cathode Composite. (a) Synthesis procedure: the $LiMn_2O_4$ cathode nanomaterial with spherical nanostructures was successfully synthesized by coprecipitation method from the reaction of lithium hydroxide and manganese acetate. A stoichiometric amount of LiOH and $Mn(CH_3COO)_2$ with the cationic ratio of Li/Mn = 1 : 2 were dissolved in deionized water by stirring gently. The solution was evaporated at 100°C for 10 h to obtain the precursor powder. The precursor was calcined at 600°C for 10 h to form the semicrystallite $LiMn_2O_4$ powder. The product was subjected to acid treatment in 2 M H_2SO_4 for 2 h to increase the degree of oxidation and remove remnant Mn_2O_3 and Mn_3O_4. (b) Coating strategy:the Pd-based bimetallic nanoparticles were prepared via an emulsion-assisted synthetic strategy. For surface modification, the Pd-Au nanoparticles and crystalline $LiMn_2O_4$ were added to deionized water and heated at 100°C under stirring until the solvent fully evaporated [17]. The well mixed powder was then calcinated at 500°C for 10 h in air. The reaction forms a solid composite of $Li(M)_xMn_{2-x}O_4$ ($x = 0.02$) which contributes to structural stability [18].

2.2. Preparation of $LiM_xMn_{2-x}O_4$ Cathode Coin Cells. The cathode was prepared by mixing 80 wt% of the pure and $Li[PdAu]_{0.02}Mn_{1.98}O_4$ active composite material, respectively, with 15 wt% acetylene black (current collector) and 5 wt% polyvinylidene fluoride binder (PVDF, dissolved in N-methyl-2-pyrrolidone, NMP) to form a slurry. The typical mass loading of active material was ~2 mg/cm^2. The slurry was then cast on the aluminium foil and cathode disks with a diameter of 12 mm were punched out and dried for 24 hours at 120°C. Test cells (LR2032, 20 d × 3.2 mm) were assembled and sealed in an Argon-filled glove box. The electrolyte used was 1 M $LiPF_6$ in ethylene carbonate (EC) : dimethyl carbonate (DMC) in a 1 : 1 volume ratio and Celgard 2400 polyethylene/polypropylene as the separator.

2.3. Characterization. The shape and size of the microstructure of $Li[PdAu]_{0.02}Mn_{1.98}O_4$ cathode were observed using a Hitachi model X-650 scanning electron microanalyser and a Tecnai G^2 F20 X-Twin MAT 200 kV transmission electron microscope. The samples were characterized by X-ray powder diffraction (XRD), which was recorder on a BRUKER AXS (Germany), D8 Advance diffractometer, using Cu-Kα radiation ($\lambda K\alpha_1 = 1.5406$ Å). The diffraction patterns were taken at room temperature in the range of $5 < 2\theta < 90^\circ$ using step scans. All electrochemical measurements used for characterization were carried out using a coin cell. Electrochemical impedance measurements were recorded with a Zahner IM6ex (Germany) workstation, at a perturbation amplitude of 10 mV within a frequency range of 100 kHz to 100 mHz. All potentials given in this paper refer to Li/Li^+.

3. Results and Discussions

The SEM micrograph of the spinel $LiMn_2O_4$ is shown in Figure 1. The pure $LiMn_2O_4$ have apparent primary particles around 50 nm and have the characteristic spinel shape. Figure 1(a) shows the secondary particles of $LiMn_2O_4$ to be about 100 nm, which are glomeration congregated tightly by primary particles, indicating that the crystals of the spinel $LiMn_2O_4$ grow very well. Well dispersed PdAu nanoparticles across the $LiMn_2O_4$ surface are shown in Figure 1(b). The $Li[PdAu]_{0.02}Mn_{1.98}O_4$ nanoparticles retained a well-developed octahedral structure with sharp edges after surface treatment with particle sizes in the range of 50–100 nm. The $Li[PdAu]_{0.02}Mn_{1.98}O_4$, having an increased surface area, favors the penetration of electrolyte, decreasing the diffusion length of lithium ions. Detailed TEM and EDX analysis of the nanoparticles shown in Figure 2(a) appear to have almost uniform spherical shape, with a tight size distribution. Figure 2(b) is an enlargement of $Li[PdAu]_{0.02}Mn_{1.98}O_4$ from which the particles appear highly crystalline. The nanocrystalline material admits electrolyte to allow rapid entry of lithium ions for quick battery charging and provide space to accommodate expansion and contraction during Li^+ intercalation and deintercalation. The diffraction pattern of the coating layer revealed that it was a single crystal with cubic spinel structure as shown in Figure 2(b) (inset). Both the $LiMn_2O_4$ and $Li[PdAu]_{0.02}Mn_{1.98}O_4$ cathodes adopt a typical spinel structure with Fd3m space group [19].

The structure of the $Li[PdAu]_{0.02}Mn_{1.98}O_4$ nanoparticles was characterized by XRD as shown in Figure 3. The X-ray diffraction pattern of $Li[PdAu]_{0.02}Mn_{1.98}O_4$ agrees with the pattern of pure $LiMn_2O_4$ and was identified as a single phase of cubic spinel with space group Fd3m. The sharp peaks and particle sizes of $Li[PdAu]_{0.02}Mn_{1.98}O_4$ as probed by XRD correlate well with the TEM analysis. No addition peaks corresponding to that of the PdAu alloy were observed in the diffraction pattern of PdAu coated $LiMn_2O_4$. The formation of a $Li[PdAu]_{0.02}Mn_{1.98}O_4$ composite structure was therefore signified by a shift (about 0.2°) in peak position to higher angles, with a slight lattice constant increase from 8.26006 Å to 8.26007 Å. This lattice expansion indicates that Pd-Au, having a larger ionic radius than Mn^{3+}, partially diffused into the crystal structure of the spinel during heat-treatment [20, 21]. The small cell parameter changes in the lattice aid the stability of the structure and the improvement of the cycle life. Chan et al. observed a similar tendency, where the substitution of Mn^{3+} with Cu^{2+}/Cu^{3+} and chromium caused an increase and decrease in lattice constant, respectively, due to the differences in ionic radii [22].

Figure 4 is the cyclic voltammograms for $LiMn_2O_4$ (a) and $Li[PdAu]_{0.02}Mn_{1.98}O_4$ (b) cycled at 0.1 mV s^{-1}. The peak separation difference suggests that the lithium intercalation

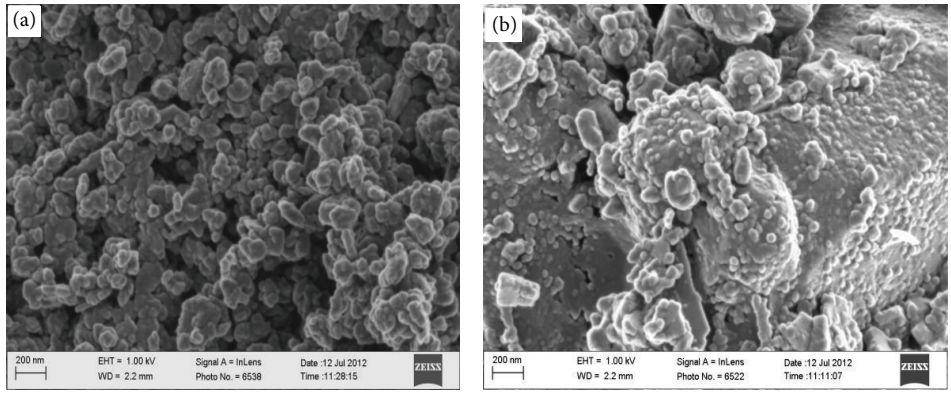

Figure 1: HRSEM of $LiMn_2O_4$ (a) and $Li[PdAu]_{0.02}Mn_{1.98}O_4$ (b) modified cathode material.

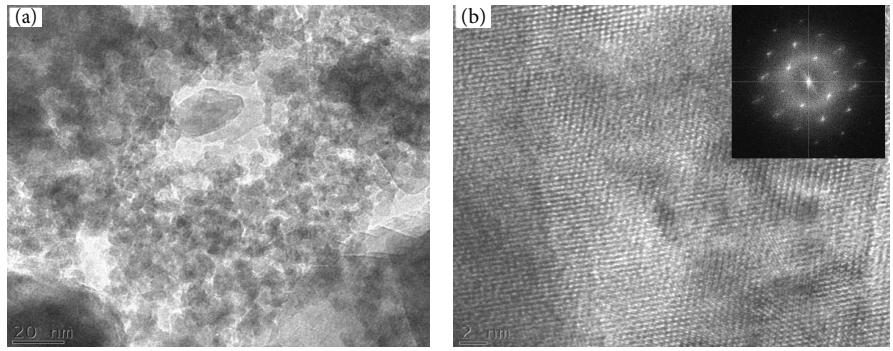

Figure 2: HRTEM of $Li[PdAu]_{0.02}Mn_{1.98}O_4$ at 20 (a) with lattice image at 2 nm (b) and electron diffraction pattern (inset).

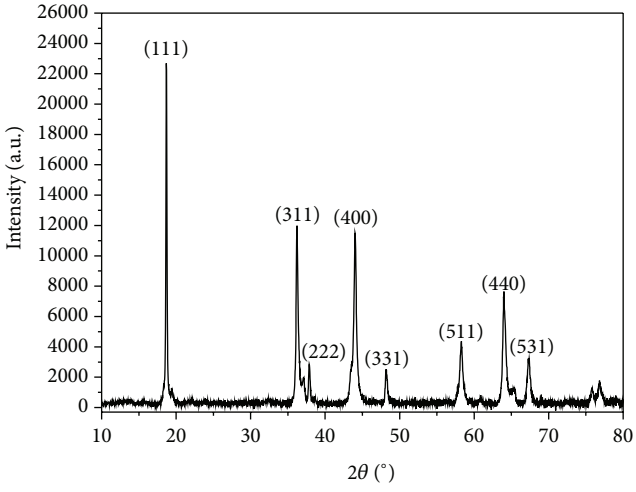

Figure 3: XRD pattern of $Li[PdAu]_{0.02}Mn_{1.98}O_4$.

and deintercalation process is much easier after modification. The two redox peak couples residing at 4.04/4.17 and 3.93/4.07 V are similar to features of voltammograms reported in [23]. The pair Pa_1/Pc_1 is attributed to the removal/addition of Li ions from/into half of the tetrahedral sites in which Li/Li interaction occurs. The Pa_2/Pc_2 pair is due to this process at the other tetrahedral sites in which lithium ions do not have any nearest neighbor Li-Li repulsive interactions [24]. These processes are accompanied by reversible Mn^{3+}/Mn^{4+} redox reactions. For $Li[PdAu]_{0.02}Mn_{1.98}O_4$, the shift in the anodic peak current to higher voltage is due to Pd-Au involvement in the prevention of Mn ion migration as a result of stronger bond strength compared to that of the Mn–O bond in the spinel structure [25]. The diffusion coefficient, D_{Li}, was 0.23 cm^2/s. and 0.63 cm^2/s. for samples (a) and (b), respectively. Faster lithium mobility in $Li[PdAu]_{0.02}Mn_{1.98}O_4$ gives rise to better high rate performances. The increased peak currents noted for $Li[PdAu]_{0.02}Mn_{1.98}O_4$ can be associated with lowered polarization and improved electrode kinetics in higher voltage region. The peak separation (0.2 V) of $Li[PdAu]_{0.02}Mn_{1.98}O_4$ was less than that of $LiMn_2O_4$, suggesting that the lithium intercalation and deintercalation process is much more efficient due to the increased sample conductivity [26]. Likewise, the total impedance as shown in Figure 5 for $Li[PdAu]_{0.02}Mn_{1.98}O_4$ was significantly lower than that of $Li[Au]_x\ Mn_{2-x}O_4$ and $LiMn_2O_4$, confirming the integration of a conducting layer. A second semicircle starts disappearing at low frequency, indicating that the two-stage intercalation/deintercalation condition of lithium varies in $Li[PdAu]_{0.02}Mn_{1.98}O_4$ [27]. The enhanced conductivity supports faster charge transportation at high current rates and is useful to prevent the pronounced pileup of Li^+ ions and undesired Mn^{3+} ions on the surfaces during discharge [28, 29]. The lower R_{ct} value obtained for $Li[PdAu]_{0.02}Mn_{1.98}O_4$

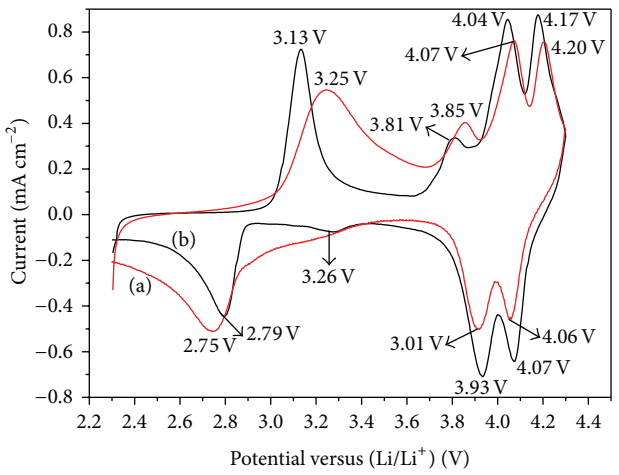

FIGURE 4: Cyclic voltammograms at 0.1 mV s^{-1} for $LiMn_2O_4$ (a) and $Li[PdAu]_{0.02}Mn_{1.98}O_4$ (b) in EC : DMC, 1 M $LiPF_6$.

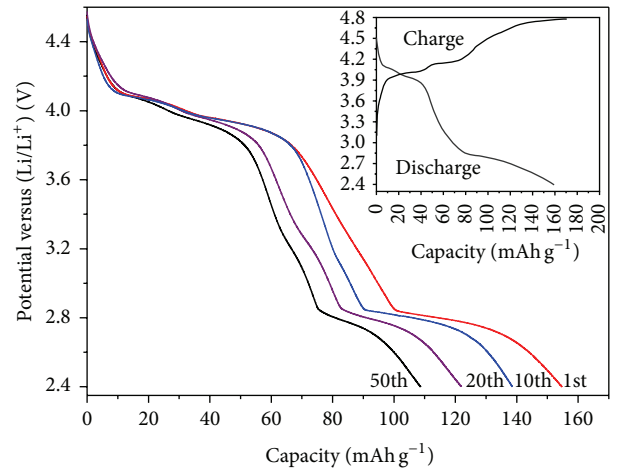

FIGURE 6: Charge/discharge curve of $Li[PdAu]_{0.02}Mn_{1.98}O_4$ cathode at 0.1 mA cm^{-2} cycled between 2.4 and 4.5 V and discharge behaviour with prolonged cycling (inset).

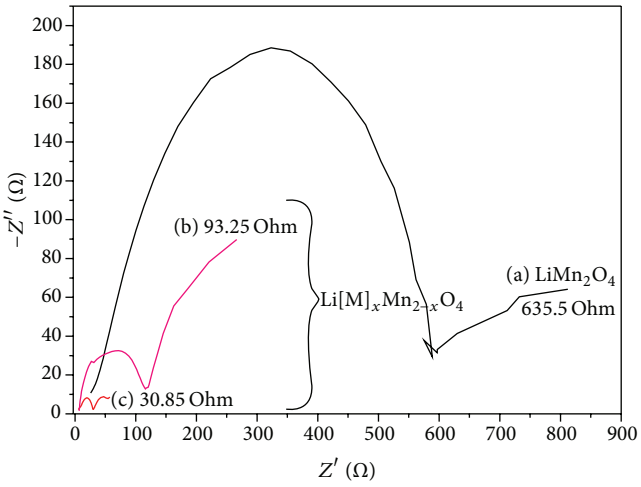

FIGURE 5: Impedance spectra of $Li[PdAu]_{0.02}Mn_{1.98}O_4$ (c), $Li[Au]_{0.02}Mn_{1.98}O_4$(b), and $LiMn_2O_4$ (a) measured at 4.5 V.

is suggestive of faster electron transfer kinetics. The capacitance, C_{dl}, value of samples (a), (b), and (c) increased steadily with values of 1.09, 2.45, and 3.05 μF. The latter is due to the presence of Pd-Au on the sample surface (in agreement with SEM observation) [30]. The exchange current i_0 followed a similar trend, with values of 1.83×10^{-4}, 2.75×10^{-4}, and 8.32×10^{-4} A cm^{-2}, which further confirmed the synergistic catalytic effect of Pd-Au with $LiMn_2O_4$.

To evaluate the cathode cycling behavior, conditions of up to 50 cycles were performed, using 0.1 C charge/discharge rates. Figure 6 shows the initial discharge capacity of $Li[PdAu]_{0.02}Mn_{1.98}O_4$ at 160.0 mAh g^{-1} which drops to 149 mAh g^{-1} after the first 50 cycles. The Pd-Au content is therefore sufficient, as it does not form a barrier but instead promotes lithium-ion movement, which enhances the initial specific capacity [31]. The discharge curves for $Li[PdAu]_{0.02}Mn_{1.98}O_4$ cell show a decrease of the effective capacity of the cell with increased cycling. This is called the capacity offset and the effect is common to most cell chemistries. The inset shows the charge/discharge curve of $Li[PdAu]_{0.02}Mn_{1.98}O_4$ cycled at a current density of 14.8 mA g^{-1} (0.1 C rate) in the potential range 2.4/4.8 V. The specific capacity of $LiMn_{2-x}O_4$ coated with Pd-Au$_x$ (in smaller quantity) shows significant improvement in the cycling performance and activity when compared with other surface doping elements for $LiMn_2O_4$ [32, 33]. The two pseudoplateaus at around 3.9 and 4.2 V represent the (redox current peaks at the positively or negatively going voltammetry curves) electrochemical behaviour of spinel $LiMn_2O_4$ [34]. The respective discharge pattern correlates with the order of atom orientation in the structure which affects the charge/discharge cycling performance [35].

4. Conclusions

Novel transition metal alloy (M_x = Pd-Au) coated $LiMn_2O_4$ with improved high rate performances have been successfully designed and synthesized using a simple coating strategy. The present study is conceivably the first time that effects of Pd-Au transition metal coating on spinel-structured $LiMn_2O_4$ are being explored. The $Li[PdAu]_{0.02}Mn_{1.98}O_4$ cathode exhibited improved rate capabilities and high rate cyclic performances compared to the pristine $LiMn_2O_4$. These improvements are due to the enhanced electronic conductivity and lithium diffusivity resulting from transition metal alloy coating. Although Pd and Au are deemed expensive for large scale industrial applications, they are uniquely durable, hence being economically viable. The [Pd-Au]-$LiMn_2O_4$ modification may be a suitable approach for producing lithium-ion battery cathodes with improved electrochemical characteristics.

Conflict of Interests

The authors declare that there is no conflict of interests regarding the publication of this paper.

Acknowledgment

This paper was financially supported by South Africa's National Research Foundation (NRF).

References

[1] P. Poizot, S. Laruelle, S. Grugeon, L. Dupont, and J.-M. Tarascon, "Nano-sized transition-metal oxides as negative-electrode materials for lithium-ion batteries," *Nature*, vol. 407, no. 6803, pp. 496–499, 2000.

[2] M. V. Reddy, G. V. Subba Rao, and B. V. R. Chowdari, "Metal oxides and oxysalts as anode materials for Li ion batteries," *Chemical Reviews*, vol. 113, no. 7, pp. 5364–5457, 2013.

[3] J. R. Dahn, U. von Sacken, M. W. Juzkow, and H. Al-Janaby, "Rechargeable $LiNiO_2$/carbon cells," *Journal of the Electrochemical Society*, vol. 138, no. 8, pp. 2207–2211, 1991.

[4] G. T. K. Fey, K. S. Wang, and S. M. Yang, "New inverse spinel cathode materials for rechargeable lithium batteries," *Journal of Power Sources*, vol. 68, no. 1, pp. 159–165, 1997.

[5] M. M. Thackeray, W. I. F. David, P. G. Bruce, and J. B. Goodenough, "Lithium insertion into manganese spinels," *Materials Research Bulletin*, vol. 18, no. 4, pp. 461–472, 1983.

[6] H. D. Abruna, Y. Kiya, and J. C. Henderson, "Batteries and electrochemical capacitors," *Physics Today*, 2008.

[7] M. Prabu, M. V. Reddy, S. Selvasekarapandian, G. V. Subba Rao, and B. V. R. Chowdari, "(Li, Al)-co-doped spinel, $Li(Li_{0.1}Al_{0.1}Mn_{1.8})O_4$ as high performance cathode for lithium ion batteries," *Electrochimica Acta*, vol. 88, pp. 745–755, 2013.

[8] R. Malik, A. Abdellahi, and G. Ceder, "A critical review of the Li insertion mechanisms in $LiFePO_4$ electrodes," *Journal of the Electrochemical Society*, vol. 160, no. 5, pp. A3179–A3197, 2013.

[9] J. Guan and M. Liu, "Transport properties of $LiMn_2O_4$ electrode materials for lithium-ion batteries," *Solid State Ionics*, vol. 110, no. 1-2, pp. 21–28, 1998.

[10] T. Teranishi and M. Miyake, "Size control of palladium nanoparticles and their crystal structures," *Chemistry of Materials*, vol. 10, no. 2, pp. 594–600, 1998.

[11] X. Sun, H. S. Lee, X. Q. Yang, and J. McBreen, "Improved elevated temperature cycling of $LiMn_2O_4$ spinel through the use of a composite LiF-based electrolyte," *Electrochemical and Solid-State Letters*, vol. 4, no. 11, pp. A184–A186, 2001.

[12] S.-T. Myung, S. Komaba, and N. Kumagai, "Enhanced structural stability and cyclability of Al-doped $LiMn_2O_4$ spinel synthesized by the emulsion drying method," *Journal of the Electrochemical Society*, vol. 148, no. 5, pp. A482–A489, 2001.

[13] M. Saitoh, S. Yoshida, H. Yamane et al., "Capacity fading of the acid-treated lithium manganese oxides in high-temperature storage," *Journal of Power Sources*, vol. 122, no. 2, pp. 162–168, 2003.

[14] T. Kakuda, K. Uematsu, K. Toda, and M. Sato, "Electrochemical performance of Al-doped $LiMn_2O_4$ prepared by different methods in solid-state reaction," *Journal of Power Sources*, vol. 167, no. 2, pp. 499–503, 2007.

[15] Z. Liu, W.-L. Wang, X. Liu, M. Wu, D. Li, and Z. Zeng, "Hydrothermal synthesis of nanostructured spinel lithium manganese oxide," *Journal of Solid State Chemistry*, vol. 177, no. 4-5, pp. 1585–1591, 2004.

[16] S. Ajaikumar, J. Ahlkvist, W. Larsson et al., "Oxidation of α-pinene over gold containing bimetallic nanoparticles supported on reducible TiO_2 by deposition-precipitation method," *Applied Catalysis A: General*, vol. 392, no. 1-2, pp. 11–18, 2011.

[17] S.-X. Zhao, Y.-D. Li, H. Ding, B.-H. Li, and C.-W. Nan, "Structure and electrochemical performance of $LiFePO_4$/C cathode materials coated with nano Al_2O_3 for lithium-ion battery," *Journal of Inorganic Materials*, vol. 28, no. 11, pp. 1265–1269, 2013.

[18] C. Villevieille, C. M. Ionica-Bousquet, A. de Benedetti et al., "Self supported nickel antimonides based electrodes for Li ion battery," *Solid State Ionics*, vol. 192, no. 1, pp. 298–303, 2011.

[19] Y.-J. Li, H. Xu, L. Kong et al., "Synthesis and electrochemical characterizations of co-doped lithium manganese oxide spinel $Li_{1.035}Mn_{1.965}O_4$," *Journal of Inorganic Materials*, vol. 29, pp. 661–666, 2014.

[20] J. Tu, X. B. Zhao, G. S. Cao, D. G. Zhuang, T. J. Zhu, and J. P. Tu, "Enhanced cycling stability of $LiMn_2O_4$ by surface modification with melting impregnation method," *Electrochimica Acta*, vol. 51, no. 28, pp. 6456–6462, 2006.

[21] G. Shen, M. Xu, and Z. Xu, "Double-layer microwave absorber based on ferrite and short carbon fiber composites," *Materials Chemistry and Physics*, vol. 105, no. 2-3, pp. 268–272, 2007.

[22] H.-W. Chan, J.-G. Duh, S.-R. Sheen, S.-Y. Tsai, and C.-R. Lee, "New surface modified material for $LiMn_2O_4$ cathode material in Li-ion battery," *Surface & Coatings Technology*, vol. 200, no. 5-6, pp. 1330–1334, 2005.

[23] P. Shen, D. Jia, Y. Huang, L. Liu, and Z. Guo, "$LiMn_2O_4$ cathode materials synthesized by the cellulose-citric acid method for lithium ion batteries," *Journal of Power Sources*, vol. 158, no. 1, pp. 608–613, 2006.

[24] N. Kamarulzaman, R. Yusoff, N. Kamarudin et al., "Investigation of cell parameters, microstructures and electrochemical behaviour of $LiMn_2O_4$ normal and nano powders," *Journal of Power Sources*, vol. 188, no. 1, pp. 274–280, 2009.

[25] M. Nakayama, M. Kaneko, and M. Wakihara, "First-principles study of lithium ion migration in lithium transition metal oxides with spinel structure," *Physical Chemistry Chemical Physics*, vol. 14, no. 40, pp. 13963–13970, 2012.

[26] S.-Y. Chung, J. T. Bloking, and Y.-M. Chiang, "Electronically conductive phospho-olivines as lithium storage electrodes," *Nature Materials*, vol. 1, no. 2, pp. 123–128, 2002.

[27] J. Liu and A. Manthiram, "Understanding the improved electrochemical performances of Fe-substituted 5 V spinel cathode $LiMn_{1.5}Ni_{0.5}O_4$," *The Journal of Physical Chemistry C*, vol. 113, no. 33, pp. 15073–15079, 2009.

[28] S. B. Park, W. S. Eom, W. I. Cho, and H. Jang, "Electrochemical properties of $LiNi_{0.5}Mn_{1.5}O_4$ cathode after Cr doping," *Journal of Power Sources*, vol. 159, no. 1, pp. 679–684, 2006.

[29] D. K. Kim, P. Muralidharan, H.-W. Lee et al., "Spinel $LiMn_2O_4$ nanorods as lithium ion battery cathodes," *Nano Letters*, vol. 8, no. 11, pp. 3948–3952, 2008.

[30] Y. Xia, H. Noguchi, and M. Yoshio, "Differences in electrochemical behavior of $LiMn_2O_4$ and $Li_{1+x}Mn_2O_4$ as 4-V Li-cell cathodes," *Journal of Solid State Chemistry*, vol. 119, no. 1, pp. 216–218, 1995.

[31] J. T. Son, H. G. Kim, and Y. J. Park, "New preparation method and electrochemical property of $LiMn_2O_4$ electrode," *Electrochimica Acta*, vol. 50, no. 2-3, pp. 453–459, 2004.

[32] S. H. Guo, X. M. He, Q. X. Zeng, C. Y. Jiang, and C. R. Wan, "Preparation and electrochemical properties of spherical $LiMn_2O_4$ surface doped with cobalt," *New Chemical Materials*, vol. 35, pp. 34–36, 2007.

[33] L. Q. Zhang, T. Yabu, and I. Taniguchi, "Synthesis of spherical nanostructured $LiMxMn_{2-x}O_4$ (M = Ni^{2+}, Co^{3+}, and Ti^{4+}; $0 \leq x \leq 0.2$) via a single-step ultrasonic spray pyrolysis method and their high rate charge-discharge performances," *Materials Research Bulletin*, vol. 44, no. 3, pp. 707–713, 2009.

[34] D. Aurbach, K. Gamolsky, B. Markovsky et al., "Study of surface phenomena related to electrochemical lithium intercalation into Li_xMO_y host materials (M = Ni, Mn)," *Journal of the Electrochemical Society*, vol. 147, no. 4, pp. 1322–1331, 2000.

[35] R. J. Pei, Z. L. Cheng, E. K. Wang, and X. R. Yang, "Amplification of antigen-antibody interactions based on biotin labeled protein-streptavidin network complex using impedance spectroscopy," *Biosensors and Bioelectronics*, vol. 16, no. 6, pp. 355–361, 2001.